

Nanoparticle sensor for label free detection of swine DNA in mixed biological samples

This article has been downloaded from IOPscience. Please scroll down to see the full text article.

2011 Nanotechnology 22 195503

(<http://iopscience.iop.org/0957-4484/22/19/195503>)

View [the table of contents for this issue](#), or go to the [journal homepage](#) for more

Download details:

IP Address: 58.27.57.116

The article was downloaded on 19/09/2011 at 03:37

Please note that [terms and conditions apply](#).

Nanoparticle sensor for label free detection of swine DNA in mixed biological samples

M E Ali¹, U Hashim¹, S Mustafa², Y B Che Man², M H M Yusop²,
M F Bari³, Kh N Islam⁴ and M F Hasan⁵

¹ Institute of Nano Electronic Engineering (INNE), Universiti Malaysia Perlis, Lot 104-108, Tingkat 1, Block A, Taman Pertiwi Indah, Jalan Kangar-Alor Star, Seriab, 01000 Kangar, Perlis, Malaysia

² Halal Products Research Institute, Universiti Putra Malaysia, 43400 UPM Serdang, Selangor, Malaysia

³ School of Materials Engineering, University Malaysia Perlis, Seriab 01000, Kangar, Perlis, Malaysia

⁴ Department of Preclinical Sciences, Faculty of Veterinary Medicine, Universiti Putra Malaysia, 43400 UPM Serdang, Selangor, Malaysia

⁵ Department of Crop Science, Faculty of Agriculture, Universiti Putra Malaysia, 43400 UPM Serdang, Selangor, Malaysia

E-mail: uda@unimap.edu.my

Received 23 November 2010, in final form 1 March 2011

Published 23 March 2011

Online at stacks.iop.org/Nano/22/195503

Abstract

We used 40 ± 5 nm gold nanoparticles (GNPs) as colorimetric sensor to visually detect swine-specific conserved sequence and nucleotide mismatch in PCR-amplified and non-amplified mitochondrial DNA mixtures to authenticate species. Colloidal GNPs changed color from pinkish-red to gray-purple in 2 mM PBS. Visually observed results were clearly reflected by the dramatic reduction of surface plasmon resonance peak at 530 nm and the appearance of new features in the 620–800 nm regions in their absorption spectra. The particles were stabilized against salt-induced aggregation upon the adsorption of single-stranded DNA. The PCR products, without any additional processing, were hybridized with a 17-base probe prior to exposure to GNPs. At a critical annealing temperature (55 °C) that differentiated matched and mismatched base pairing, the probe was hybridized to pig PCR product and dehybridized from the deer product. The dehybridized probe stuck to GNPs to prevent them from salt-induced aggregation and retained their characteristic red color. Hybridization of a 27-nucleotide probe to swine mitochondrial DNA identified them in pork–venison, pork–shad and venison–shad binary admixtures, eliminating the need of PCR amplification. Thus the assay was applied to authenticate species both in PCR-amplified and non-amplified heterogeneous biological samples. The results were determined visually and validated by absorption spectroscopy. The entire assay (hybridization plus visual detection) was performed in less than 10 min. The LOD (for genomic DNA) of the assay was $6 \mu\text{g ml}^{-1}$ swine DNA in mixed meat samples. We believe the assay can be applied for species assignment in food analysis, mismatch detection in genetic screening and homology studies between closely related species.

(Some figures in this article are in colour only in the electronic version)

1. Introduction

Selective detection of specific DNA sequences is increasingly important to address a wide range of biological issues such as bio-diagnostics, genetics [1–3] and food analysis [4–10].

The polymerase chain reaction (PCR) is widely used to selectively amplify a segment of longer DNA from as little as a single copy to easily detectable quantities. The application of PCR addresses sensitivity issues and ameliorates sample purification steps [3]. For these convenient features, PCR

has become an indispensable tool for the analysis of genomic DNA [3], although a vast range of sensing approaches, such as surface plasmon resonance (SPR) [11], fluorescent microarrays [12, 13], semiconductor, nanoparticle or polymer-based biosensors [14–18], are available. The merit of a PCR-amplified assay is not sensitivity but simplicity, because additional amplification is straightforward. However, the authentication of PCR product needs further identification of specific sequences within it. Most of the sequence identification tools, available to hand, require expensive instrumentation or complicated synthetic chemistry to modify the DNA, substrates or nanoparticles. However, hybridization on modified surfaces imposes unnecessary steric constraints, leading to slow and inefficient binding of probe and target, making the analysis of PCR products expensive and time consuming [3].

Species assignment in food products is necessary for the enforcement of labeling regulations and health, and religious concern over certain food ingredients [5–10]. To perform this task, cost-effective, easily-performable and accurate analytical methods are highly desirable [7]. Recently a number of PCR assays have been developed for the detection of swine DNA in raw and processed meat [5, 6, 9], since pork is a concern for Muslims, Jews and vegans. PCR assay with shorter amplicon size (<150 bp) is preferred as it is implicated as providing higher template DNA stability in physically and chemically processed food products [10]. However, shorter amplicon size often produces cross-species amplification and artifacts diminishing the reliability of the PCR assay [10]. Generally, RFLP analysis is performed to overcome specificity issues [9]. However, RFLP involves the additional cost of restriction enzymes, digestion time and gel electrophoresis [9]. Moreover, RFLP cannot be applied if restriction sites are not present in the desired PCR products. Thus the analysis of PCR product is complex and it considerably hinders the transition of the method from research to routine analysis of consumer goods [19, 20]. Therefore, new methods with convenient features would be greatly appreciated for the accurate analysis of PCR-amplified DNAs.

The distinct surface plasmon resonance (SPR) characters of aggregated and non-aggregated gold nanoparticles with diameter 5–20 nm have been studied for many years for sensing specific oligonucleotide sequences [15–17, 20–33]. However, those studies involved a cross-linking mechanism which needs surface modification of GNPs to immobilize two DNA probes that are subsequently cross-linked by a complementary target to induce aggregation [22–26].

Detection of nucleotide sequences by a non-cross-linking method is particularly interesting because it needs no modification chemistry and target hybridization is rapid as well [3, 17]. Li *et al* showed that 13 nm GNPs can be applied to detect specific sequences and single nucleotide mismatch in PCR-amplified DNA [3]. Mismatch detection in genomic DNA is a challenging task but is at the forefront of diagnostic technology for the early detection of cancers and other hereditary diseases [34, 35]. However, such studies are also limited to a definite size of colloidal gold and lack substantial evidence from absorption spectroscopy, which is

a reliable and inexpensive tool available in most laboratories. It is not clear whether other than 13 nm diameter GNPs can be used for sequence identification schemes. It also needs to be clarified whether GNPs can be used to directly detect PCR-non-amplified genomic DNA where sample scarcity is not a concern. Application of unmodified GNPs for the authentication of specific sequences in heterogeneous biological samples also needs to be explored.

This work successfully applied 40 ± 5 nm GNPs for visual differentiation of shorter size PCR amplicons (109 bp) of pig and deer cytb genes, avoiding any surface modification chemistry or RFLP analysis. Thus we showed that colloidal gold of wide ranging diameter could be used to simplify the analysis of PCR products. The visually observed results were substantiated by absorption spectroscopy and electron microscopy. These eliminated the probability of artifacts or any sort of color blindness errors. The assay also directly detected swine DNA in genomic DNA mixtures extracted from moderately processed pork–venison and pork–shad binary admixtures, avoiding the additional cost and time of PCR amplification, electrophoresis and sample purification chemistry.

2. Materials and methods

2.1. PCR amplification

Out of eleven species (pork/pig: *Sus scrofa*, beef/cow: *Bos taurus*, chevon/goat: *Capra hircus*, mutton/sheep: *Ovis aries*, venison/deer: *Cervus nippon* and chicken: *Gallus gallus*) and fish (cichlid: *Crenicichla minuwano*, shad: *Alosa sapidissima*, cod shrimp: *Gadus morhua*, bluefin tuna: *Thunnus orientalis* and cuttlefish: *Sepia officinalis*), 109 bp size PCR products were obtained from pig, deer and shad cytb genes. DNAs of these species were extracted from fresh and autoclaved (at 120 °C for 30 min) muscle tissue using MasterPure™ DNA Purification Kit (Epicenter Biotechnologies, Madison, USA) as per the protocol supplied by the manufacturer. The purity and concentration were determined by Eppendorf UV–vis Biophotometer (Eppendorf, Germany). The fresh muscle samples were procured from a local wet market and were verified by veterinary and fishery experts. Primers and probes (table 1) were designed by analyzing *Sus scrofa* cytb gene (GenBank # AF034253.1 in NCBI archive) using NCBI BLAST, ClustalW alignment and primer3Plus software. The cycling conditions on a Mastercycler Gradient PCR (Eppendorf, Germany) were: preheating at 95 °C for 10 min, 35 cycles of amplification (30 s at 93 °C, 20 s annealing at 61 °C and 30 s extension at 72 °C) followed by final extension at 72 °C for 5 min. The PCR products were analyzed by electrophoresis on 2% agarose gel for 75 min at 50 V and were visualized by ethidium bromide staining [4, 6].

2.2. Synthesis of colloidal gold nanoparticles

Colloidal gold nanoparticles (GNPs) were synthesized with a slight modification of the method described in the literature [21]. Instead of tri-sodium citrate, 38.8 mM solution of monobasic anhydrous sodium citrate (MW. 214.11, 99.5%)

Table 1. Sequences of oligonucleotides used.

Name	Sequence (5'–3')
Forward primer	TCCTGCCCTGAGGACAAATA
Reverse primer	AAGCCCCCTCAGATTCATTC
Swine probe for genomic DNA	CTACGGTCATCACAAATCTACTATCAG
Swine probe for PCR product	<u>CTACGGTCATCACAAAT</u>
PCR amplicon	TCCTGCCCTGAGGACAAATATCATTCTGAGGAG <u>CTACGGTCATCACAAAT</u> CTACTATCAGCTATCCCTTAT AT CGGAACAGACCTCGTAGAATGAATCTGAGGGGGCTT

was used in this preparation. All chemicals were purchased from Sigma, Aldrich, USA, and all solutions were prepared in 18.2 MΩ water immediately before use. The resultant GNPs were characterized by PerkinElmer Lambda 25 UV–vis spectrophotometer and Hitachi 7100 transmission electron microscope. The concentration and particle number were determined according to the method of Heiss *et al* [36].

2.3. Identification of PCR product by gold nanoparticles

In four separate vials, labeled as (a)–(d) (figure 3), 400 μl of 66 pM colloidal GNPs was taken. Thirty microliter (30 μl) of 17-mer single-stranded (ss-) and double-stranded (ds-) oligo-probes (100 nM) (1st BASE, Malaysia) were added to vials (c) and (d). An equal volume of 18.2 MΩ water was added to vials (a) and (b). All vials were incubated in a water bath at 50 °C for 3 min, except the dsDNA-containing vial (vial (d)) to avoid temperature-induced dehybridization of the complementary strands. Then 200 μl of 10 mM PBS buffer (0.2 M NaCl, pH 7.4) was added to each tube, except vial (a) in which equal volume of 18.2 MΩ water was added. All tubes were vortexed immediately. The colloidal suspension in PBS buffer (vial (b)) and dsDNA (vial (d)) immediately turned purple-gray and then slowly watery-gray. However, GNPs in DI water (vial (a)) and first incubated in ssDNA and then in PBS buffer remained unchanged and retained their characteristic pinkish-red color (vial (c)). After 10 min, sufficient water was added to make the final volume 1 ml in each vial and was characterized by absorption spectroscopy. Thus the final concentration of probe, GNPs and PBS buffer was 3 nM, 26.4 pM and 2 mM, respectively. Stability of ssDNA incubated gold colloids in PBS buffer was studied for seven days, keeping them at 4 °C, and found unchanged. Replacement of synthetic dsDNA by PCR product yielded similar results. The samples were also characterized by transmission electron microscopy (figure 2) in the Institute of Biosciences in the University Putra Malaysia.

2.4. Sequence identification and mismatch detection by gold colloids

For Sequence identification and mismatch detection, 40 μl porcine PCR products (500 μg ml⁻¹) and 30 μl of 17-mer swine probes (100 nM) were taken in vials (a), (c) and (e) (figure 4). Equal volumes of deer PCR product and probes were taken in vials (b), (d) and (f). The mixtures were denatured at 95 °C for 3 min and then annealed at 51 °C ((a), (b)), 55 °C ((c), (d)) and 59 °C ((e), (f)) for 2 min.

Finally, 400 μl of 66 pM gold colloids were added to each vial. At 51 °C, gold colloids in both PCR products immediately turned purple-gray (vials (a) and (b) in figure 4). At 55 °C, the colloidal particles in deer PCR product (vial (d)) retained their characteristic pinkish-red color. However, the particles in porcine PCR product turned purple-gray (vial (c)). At 59 °C the pinkish-red color was retained by both PCR products (vials (e), (f)). The final volume was adjusted to 1 ml with DI water and characterized by UV–vis spectroscopy. Thus the final concentration of colloidal particles, ssDNA probe and PCR products were 26.4 pM, 3 nM and 20 μg ml⁻¹, respectively.

2.5. Detection of swine DNA in mixed meat mixture

In order to detect swine DNA in moderately processed heterogeneous biological samples, pork–venison, pork–shad and shad–venison mixtures were prepared in a ratio of 1:1 (w/w). Approximately 100 mg mixed and pure meat samples from each specimen were autoclaved at 120 °C for 30 min at a pressure of 3 bar. By this treatment, all specimens lost their normal textures and turned into a liquid broth. DNA extraction was performed as described in section 2.1. One hundred microliters (100 μl) of mixed genomic DNA (200 μg ml⁻¹) was taken in vials (b)–(d) as shown in figure 5. Equal amounts of pure genomic DNA (pig, deer and shad) were taken in vials (a), (e) and (f). All vials were incubated with 15 μl of (100 nM) swine probe (27-nucleotide shown in table 1) at 95 °C for 3 min and then annealed at 55 °C for 2 min. After that, 250 μl of 66 pM gold colloids was added to each vial. Finally, 100 μl of 10 mM PBS was added to each vial. Vials (a)–(c), which contained swine DNA, immediately turned purple-gray. However, the remaining vials, which did not contain any swine DNA, retained the characteristic color of colloidal particles. The final volume was made up to 1 ml with DI water and characterized by absorption spectroscopy. Thus the final concentration of GNP, probe, genomic DNA and PBS was 16.5 pM, 1.5 nM, 20 μg ml⁻¹ and 1 mM, respectively.

2.6. Determination of the limit of detection

To determine the LOD (limit of detection), raw pork and venison was mixed in a ratio of 1:99; 10:90; 20:80 and 30:70 (w/w). DNA extraction was performed from the mixed meat and 100 μl of mixed DNA (300 μg ml⁻¹), extracted from the above specimens, was taken in four separate vials marked as (a)–(d), as shown in figure 6. All vials were incubated with 15 μl of (100 nM) swine probe (27-nucleotide shown in

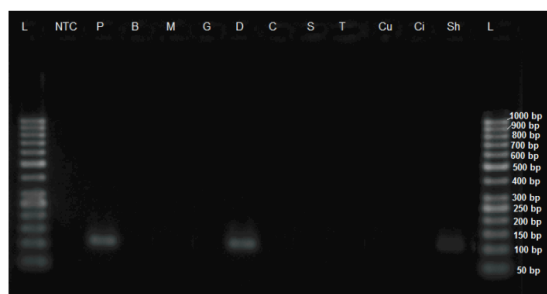


Figure 1. Electrophoresis analysis of PCR products of eleven different species. Shown are L: DNA ladders (50–1000 bp); P: pork, B: beef, M: mutton, G: goat, D: deer, C: chicken, S: shrimp, T: tuna, Cu: cuttlefish, Ci: cichlid, Sh: shad and NTC: negative template control.

table 1) at 95 °C for 3 min and then annealed at 55 °C for 2 min. After that 250 μ l of 66 pM gold colloids was added to each vial. Finally, 100 μ l of 10 mM PBS was added to each vial. Vial (a) retained the pinkish-red color of monomeric GNPs. Vials (c) and (d) clearly turned purple-gray. On the other hand, vials (b) took a mixed appearance with the retention of approximately 60–70% original color. The final volume was made up to 1 ml with DI water and was characterized by absorption spectroscopy. Thus the final concentration of probe, GNP, mixed genomic DNA and PBS were 1.5 nM, 16.5 pM, 30 μ g ml⁻¹ and 1 mM, respectively. The concentration of swine DNA in vials (a)–(d) was 0.3, 3.0, 6.0 and 9.0 μ g ml⁻¹, respectively.

3. Results and discussion

3.1. PCR amplification

PCR amplification results are shown in figure 1. Out of eleven different species, 109 bp products were obtained from pig, deer and shad cytb genes at 61 °C annealing temperature. However, the amount of shad PCR product was significantly less than the deer product. Sequence analysis revealed that the forward primer has a 2 nucleotide (2-nt) mismatch with both deer and shad templates (data not shown). So the DNA of both species should amplify at the same level at the same annealing temperature. However, replacement of C with T at the second position brought two T at the beginning of the shad primer, probably making the primer hybridization difficult at high temperature. Other species produced (goat, cow, sheep, chicken, shrimp, cichlid, cuttlefish and tuna) no product at all, because they had a 3–9 nucleotide mismatch with the primers and therefore, the primers did not hybridized to the template at the experimental annealing temperature.

3.2. Characterization of gold nanoparticles

The formation of gold nanoparticles was confirmed by TEM images (figure 2). The particle size (diameter: 40 \pm 5 nm) was assigned according to previously established methods [3, 37, 38]. TEM images (2(A) and (C)) revealed the distribution of particles in small monodisperse groups

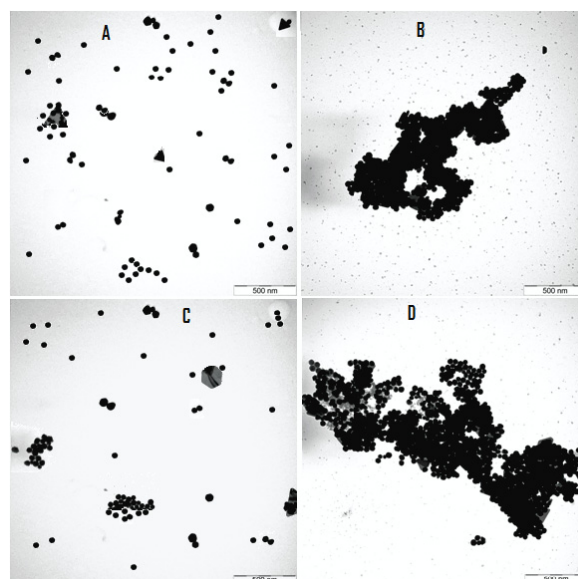


Figure 2. TEM images of gold nanoparticles (GNPs) before and after salt-induced aggregation. Shown are 26.4 pM gold colloids in DI water (A), in 2 mM PBS buffer (B) in 2 mM PBS after 3 min incubation in ssDNA probe (3 nM) at 50 °C (C) and in 2 mM PBS after the same duration incubation in equimolar 17-mer dsDNA at 25 °C (D). All images are shown at a magnification of 50 000 times.

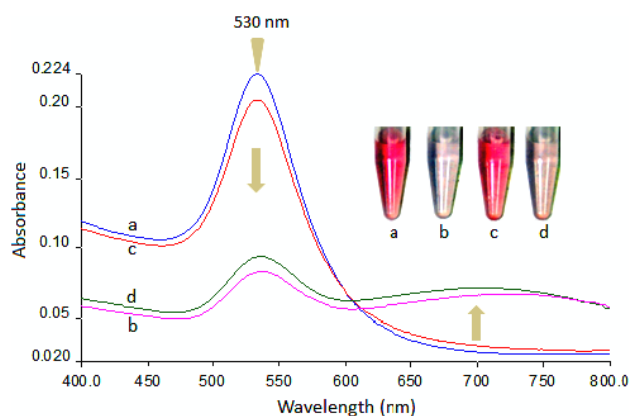


Figure 3. Absorption spectra of aggregated and non-aggregated GNPs. Shown are absorption spectra of 26.4 pM gold colloids in DI water (blue curve: top one, (a)), in 2 mM PBS buffer (pink curve: bottom one, (b)) and in 2 mM PBS buffer after incubation with ssDNA probes (red curve: second from the top, (c)), and in equimolar dsDNA probes (green curve: third from the top, (d)). Insets are the color photographs of 1.6 \times concentrated solutions in DI water (a), PBS buffer (b), PBS buffer plus ssDNA (c) and PBS buffer plus dsDNA (d).

throughout the bulk sample, but not in aggregates (one on another) that were seen upon the addition of salt (figures 2(B) and (D)). A significant portion (\sim 2–5%) of the particles was found to be triangular, rod, rhombic, hexagonal or rectangular in shape.

Previous studies implicated that tri-sodium citrate concentration [37], mixing speed [37, 38] and reaction temperatures [39, 40] critically affects the particle size and shape of monodisperse gold sols. Reduction of citrate concentration

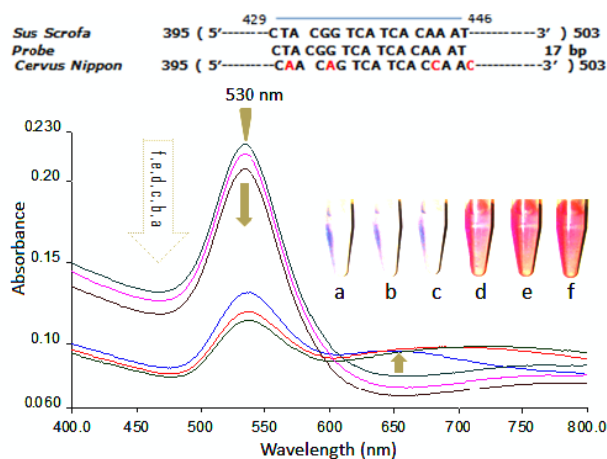


Figure 4. Identification of PCR products and nucleotide mismatch by unmodified GNPs. In the illustration vials (a), (c) and (e) represent the color of gold colloids in pig PCR product annealed with the swine probe DNA at 51, 55 and 59 °C, and vials (b), (d) and (f) shows the same in deer PCR product annealed with the same probe at the corresponding temperatures. The absorption spectra from bottom to top are green curve: pig at 51 °C (a), red curve: deer at 51 °C (b), blue curve: pig at 55 °C (c), brown curve: deer at 55 °C (d), pink curve: pig at 59 °C (e) and cyan curve: deer at 59 °C (f). The inset is the matched and mismatched sequences of pig and deer cytb genes with the designed probe. The sequence of the corresponding spectra is also shown alphabetically within the pointed arrow.

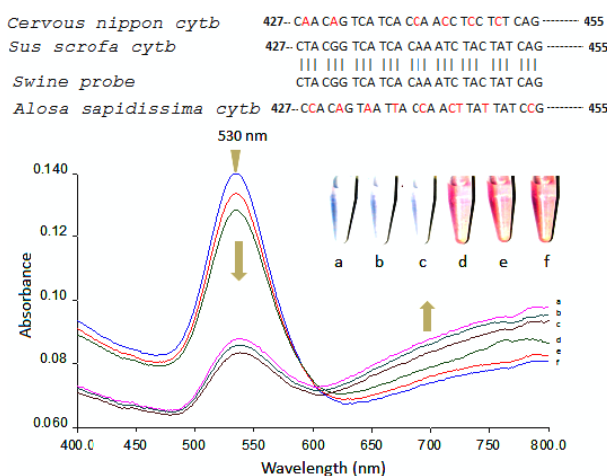


Figure 5. Identification of swine DNA in heat and pressure processed mixed genomic DNA mixtures. Vials (a), (e) and (f) contained pure genomic DNA extracted from autoclaved meat from pig, deer and shad. However, vials (b)–(d) contained mixed genomic DNA extracted from 1:1 (w/w) mixtures of pig–deer, pig–shad and deer–shad muscle tissue autoclaved under similar conditions. The corresponding absorption spectra are labeled alphabetically. All vials were incubated at 95 °C for 3 min to allow denaturation and then annealed at 55 °C for 2 min before adding the colloidal particles.

produces larger particles and enhancement of citrate generates smaller particles [37]. In place of tri-sodium citrate, mono-sodium citrate was used at a concentration (38.8 mM), at which tri-sodium citrate is reported to produce particles equal or less than 13 nm [21]. However, particles of diameter of

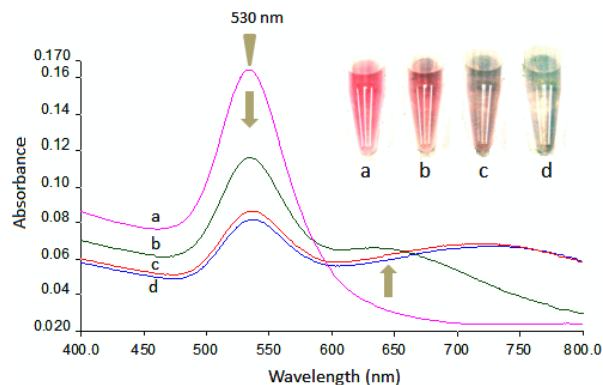


Figure 6. Determination of LOD for pork in raw pork–venison binary admixture. Shown in the inset are the color of gold nanoparticles in 1% (a), 10% (b), 20% (c) and 30% (d) pork DNA extracted from pork–venison mixture. The corresponding absorption spectra are shown with label. The LOD was found to be 20% ($6 \mu\text{g ml}^{-1}$) swine DNA in the binary mixture (shown in vial (c) and by red curve).

40 ± 5 nm were obtained in the current report. Using tri-sodium citrate under similar conditions, colloidal particles of diameter 20 ± 2 nm were found (data not shown). Thus it was inferred that the lower number of sodium ions in the monobasic sodium citrate molecule contributed to the formation of larger size particles.

UV–vis spectra of isolated and aggregated 40 ± 5 nm GNPs in DI water and 2 mM PBS are shown in figure 3. The unaggregated sol produced an intense peak at 530 nm. The physical nature of this surface plasmon mode, which gives colloidal gold its characteristic pinkish-red color, is well understood, as it depends on particle size and shape [3, 15, 16, 36, 41, 42]. For example, 13 nm GNPs produce an absorption peak at 520 nm [3, 21] whereas 2.5 nm particles produce a peak at 510 nm [16].

However, the aggregated colloidal particles in this report lost the absorption peak at 530 nm in PBS. Moreover, a well developed broad peak, which resulted from a collective plasmon mode in aggregated particles, appeared between 620 and 800 nm [3, 21]. The new features of the spectrum started to develop in the region of 650 nm and gradually red-shifted and went upward, occupying a larger part (620–800 nm), as shown in figure 4 (blue curve: fourth from the top). The intensity of the new peak was directly proportional to the degree of aggregation and loss of absorption at 530 nm (shown by arrows in figure 3).

3.3. Sequence identification and mismatch detection

Agarose gel electrophoresis coupled with ethidium bromide staining is routinely used to visualize PCR-amplified DNAs [4, 6–9]. However, gel electrophoresis is time consuming, laborious and cannot differentiate different sequence-containing PCR products if they have the same molecular size as shown in figure 1. RFLP analysis is generally done to differentiate PCR products of the same sizes [9]. However, RFLP analysis incurs the additional cost of restriction enzymes, time consuming digestion and laborious

electrophoresis. Moreover, this method can be applied only if appropriate restriction sites are present in a comparatively longer size amplicon. Southern blotting is another technique that can be used for sequence identification [43]. In addition to high cost of materials and handling of hazardous materials, such as ethidium bromide and radioactive materials, the whole process takes more than a day, reflecting the numerous disadvantages of this method. Sequencing is another technique that can identify specific PCR products [44]. However, this method demands excessively purified DNA.

On the other hand, colloidal gold is biocompatible, its chemistry is well known, its preparation is easier at desirable sizes and it is also commercially available at reasonable prices. Therefore, we proceeded to identify species specific sequences in PCR products by gold nanoparticles. We designed a 17-mers probe that had 100% matches with porcine PCR product and 4-nt mismatch with deer product (inset of figure 4). We observed that at a critical temperature (55 °C), swine-specific probe is dehybridized from the non-complementary PCR products obtained from deer *cytb* gene. The dehybridized probes (17-mer ssDNA) interact with GNPs to prevent them from aggregation after the addition of salt at a critical concentration. This produces a rapid and drastic color change in the reaction mixtures, which can be detected by visual observation (vial (c) and (d) in the inset of figure 4) without the need of any instrumental aid. Earlier works by Li *et al* [3] described the mechanism of color changes in 13 nm GNPs and their interactions with ssDNA. The procedure for determining the critical concentration of salt can be found elsewhere [37].

We validated our visually observed findings by absorption spectroscopy (figure 3). The UV-vis spectrum of GNPs in PBS lost its absorption peak at 530 nm, indicating aggregation. Salt-induced aggregation of citrate-coated particles was confirmed by TEM study (figure 2(B)). Double-stranded 17-mer DNA and also PCR product could not prevent salt-induced aggregation of GNPs. This was also confirmed by TEM study (figure 2(D)) and the loss of the 530 nm peak by 70–80% (spectrum (d) in figure 3). However, a reduced level of aggregation was observed both in the TEM image (figure 2(D)) and the UV-vis spectrum (figure 3: spectrum (d)). We assumed the presence of some ssDNA, both in synthetic dsDNA and PCR product, that might adsorb on GNP surfaces to interfere with aggregation. This was confirmed by measuring ssDNA species using a biophotometer (Eppendorf) that detected the presence of 10–15% ss-nucleic acids (DNA or RNAs) in synthetic dsDNA and PCR products as well. The UV-vis spectrum of GNPs in ssDNA produced an ~5% less intense peak at 530 nm, indicating some degree of aggregation upon the addition of salt. This was revealed by TEM study (figure 2(C)) and also by the higher base line in the region of 620–800 nm in the absorption spectrum (red curve in figure 3). Thus we were able to clearly demonstrate that absorption at 530 nm gradually decreased, and between 620 and 800 nm increased, as the particles undergo aggregation.

As shown in figure 4, the absorption spectra of gold colloids in both pig and deer PCR products (green and red curves) indicated equal levels of aggregation at 51 °C, as the absorption at 530 nm reduced and that at 620–800 nm

increased to the same extent. However, the absorption of deer PCR product (brown curve) at 530 nm was significantly increased and that between 620 and 800 nm decreased over that of pig (blue curve) at 55 °C, indicating almost complete dehybridization of the probe from deer PCR product and consequent isolation of gold colloids. However, all probes were forced to dehybridize from both PCR products at 59 °C and therefore both spectra (pink & cyan curves) were intensified at 530 nm and fell down between 620 and 800 nm to the same extent. We observed a shoulder at 650 nm for the pig PCR product at 55 °C but not for the deer product. This type of shoulder indicated partial aggregation of GNPs. Ultimately, the shoulder centered at 650, spread over the entire region of 620–800 nm when complete aggregation of particles took place. A slight variation in spectral shape and base line was observed between the samples, which could be explained for different dielectric properties of the solution due to different level of nucleic acids, proteins or other impurities in the PCR products [41, 42, 45]. A pipetting error might also contribute to the variation from experiment to experiment. However, the observed variation failed to affect our visual findings. We successfully identified specific sequences in PCR product through mismatch detection by visual observation of the color change, without the aid of any instrumentation. Absorption spectroscopy strongly supported our visual findings through monitoring the spectral intensity at 530 nm and 620–800 nm.

3.4. Sequence detection in mixed biological samples

The swine-specificity of the probes was confirmed by detecting swine DNA in binary admixtures (1:1 w/w) of pork–venison, pork–shad and deer–shad genomic DNA extracted from autoclaved mixed meat (figure 5). The purpose of autoclaving was to see whether partially degraded DNA could be detected by GNPs, as several literature reports have demonstrated that such treatment breaks down genomic DNA into small fragments [8, 10]. A certain level of genomic DNA degradation is also obvious during physical and chemical processing of meat and meat products [8, 10]. Therefore, our attempt to detect specific DNA sequences in heat-treated and pressurized meat mixture was appropriate.

We designed a comparatively longer swine-specific probe (27-nucleotide shown in table 1) for the detection of non-amplified swine genomic DNA in mixed meat samples. This probe had 6-nt and 8-nt mismatches (inset of figure 5) with deer (*Cervus nippon*; GenBank 377264.1) and shad (*Alosa sapidissima*; GenBank EU552616.1) *cytb* genes. Incubation of the probe with pure and mixed genomic DNA, followed by addition of gold colloids, clearly demonstrated that only the swine DNA-containing vials ((a)–(c)) changed color from pinkish-red to watery-gray, reflecting hybridization of the probe to the swine genomic DNA at 55 °C. No detectable change in color was observed in deer–shad mixture (d) or pure genomic DNA of deer and shad ((e) and (f)) indicating that the probe did not hybridize to mismatch containing genomic DNA under similar conditions. Again, absorption spectroscopy strongly supported the visually observed results, suggesting that the visual change of color was authentic.

3.5. Determination of LOD

The absorption spectra and visually detected color of GNPs in various percentages of pork–venison binary admixtures are shown in figure 6. It was very clear from the visually observed results, as well as spectroscopic data, that 1% pork-containing vial (vial (a)) retained 100% original color of colloidal particles (pink curve). However, 10% pork-containing vial (b) retained 60–70% color of GNPs, reflecting partial aggregation. This was also reflected by the appearance of a shoulder centered at 650 nm and the loss of absorption by 40–50% at 530 nm. On the other hand, 20% and 30% pork-containing vials ((c) and (d)) changed color from pinkish-red to purple-gray demonstrating aggregation. Absorption spectra reflected the surface plasmon features of 40 nm diameter aggregated particles between 620 and 800 nm and loss of absorption at 530 nm. Concentration of swine DNA in 20% pork-containing vial was $6 \mu\text{g ml}^{-1}$. Thus the determined LOD was $6 \mu\text{g ml}^{-1}$ swine DNA for raw pork in mixed samples. It was observed that some of the particles (~5–10%) did not change color in vials (c) and (d), which contained 20% and 30% swine DNA. These were most likely the unconsumed probe-bound particles that tolerated the salinity stress.

3.6. Efficacy and limitation of the current assay

The current assay successfully determined swine-specific sequences in PCR-amplified and non-amplified pure and mixed meat mixtures in raw as well as moderately processed states just by visually observed color change of gold nanoparticles. The visually observed results were authenticated by absorption spectroscopy. However, the assay could not provide quantitative information. The LOD of the assay was higher than that of the real-time PCR [5, 10]. The TaqMan fluorogenic probe can detect, quantify and amplify specific sequences by real-time PCR without the need of electrophoresis and blot analysis [5, 9]. However, the TaqMan probe, real-time PCR and the mastermix used in real-time PCR are very expensive and ordinary laboratories cannot afford them. On the other hand, a conventional thermal cycler is cheap and can be used to amplify target DNA sequences to overcome sample scarcity. Conventional PCR coupled with gold-nanoparticles-based sequence detection can reduce both the cost and time, and can be afforded by ordinary laboratories. UV–vis spectroscopy, which is available in most laboratories, can complement the visually identified results of colloidal gold. In addition, the developed assay can be applied to detect specific sequences without the need of PCR amplification if adequate sample is available.

4. Conclusion

A methodology for rapid (less than 10 min) and reliable detection of specific sequences and nucleotide mismatch in PCR-amplified and non-amplified DNA using aggregating properties of 40 nm gold nanoparticles as colorimetric sensor was developed. The assay was label free, required no surface functionalization chemistry, detecting instrumentation and was applicable for species assignment in food analysis. 40 nm

gold nanoparticles were prepared by a simple and easily performable method. We demonstrated that ssDNA adsorbed on these particles to stabilize them against salt-induced aggregation. The characteristic pinkish-red color of these colloidal particles was sensitive to the degree of aggregation and was monitored by absorption spectroscopy, transmission electron microscopy or simply by visual observation. The method was applied for the first time to identify specific sequences and mismatch in moderately processed mixed meat for the authentication of species. Convincing evidence for the authenticity of the visually observed results was produced by absorption spectroscopy as well as electron microscopy. The method successfully replaced some conventional analytical methods, such as gel electrophoresis, RFLP, Southern blotting or sequencing for the post-PCR analysis of PCR-amplified DNAs. Thus the beauty of the developed assay was its simplicity. We successfully identified swine DNA in heterogeneous biological samples without the aid of any instrument, even without PCR amplification.

Acknowledgments

This research was supported by the Ministry of Science, Technology and Innovation (MOSTI), Malaysia, grant no. 05-01-04-SF0285 to Professor Y B Che Man, the Ministry of Agriculture (MOA), Malaysia, grant no. SF-9006-0008 to Professor U Hashim and the Universiti Malaysia Perlis (UniMAP) Graduate Assistantship to M E Ali.

References

- [1] Rees J 2002 *Science* **296** 698–701
- [2] Hood L and Galas D 2003 *Nature* **421** 444–8
- [3] Li H and Rothberg L J 2004 *J. Am. Chem. Soc.* **126** 10958–61
- [4] Hunt D J, Parker H C and Lumley I D 1997 *Food Chem.* **60** 437–42
- [5] Rodríguez M A, García T, González I, Hernández P E and Martín R 2005 *Meat Sci.* **70** 113–20
- [6] Che Man Y B, Aida A A, Raha A R and Son R 2007 *Food Control* **18** 885–9
- [7] Ballin N Z, Vosensen F K and Karlsson A H 2009 *Meat Sci.* **83** 165–74
- [8] Arslan A, Ilhak O I and Calioglu M 2006 *Meat Sci.* **72** 326–30
- [9] Murugaiyah C, Noor Z M, Mastakim M, Bilung L M, Selamat J and Radu S 2009 *Meat Sci.* **83** 57–61
- [10] Rojas M, González I, Pavon M A, Pegels N, Lago A, Hernández P E, García T and Martín R 2010 *Food Addit. Contam.* **27** 749–63
- [11] Nelson B P, Grimsrud T E, Liles M R, Goodman R M and Corn R M 2001 *Anal. Chem.* **73** 1–7
- [12] Sueda S, Yuan J L and Matsumoto K 2002 *Bioconjug. Chem.* **13** 200–5
- [13] Paris P L, Langenhan J M and Kool E T 1998 *Nucleic Acids Res.* **26** 3789–93
- [14] Garion D, Parak W J, Williams S C, Zanchet D, Micheel C M and Alivisatos A P 2002 *J. Am. Chem. Soc.* **124** 7070–4
- [15] Dubertret B, Calame M and Libchaber A J 2001 *Nat. Biotechnol.* **19** 365–370
- [16] Maxwell D J, Taylor J R and Nie S 2002 *J. Am. Chem. Soc.* **124** 9606–12
- [17] Sato K, Hosokawa K and Maeda M 2003 *J. Am. Chem. Soc.* **125** 8102–3

- [18] Gaylord B S, Heeger A J and Bazan G C 2003 *J. Am. Chem. Soc.* **125** 896–900
- [19] Sails A D, Fox A J, Bolton F J, Wareing D R A and Greenway D L A 2003 *Appl. Environ. Microbiol.* **69** 1383–90
- [20] Belgrader P, Bennett W, Hadley D, Long G, Mariella R Jr, Milanovich F, Nasarabadi S, Nelson W, Richards J and Straton P 1998 *Clin. Chem.* **44** 2191–4
- [21] Graber K C, Freeman R G, Hommer M B and Natan M J 1995 *Anal. Chem.* **67** 735–43
- [22] Mirkin C A, Letsinger R L, Mucic R C and Storhoff J J 1996 *Nature* **382** 607–9
- [23] Alivisatos A P, Johnsson K P, Peng X G, Wilson P E, Loweth C J, Bruchez M P and Schultz P G 1996 *Nature* **382** 609–11
- [24] Elghanian R, Storhoff J J, Mucic R C, Letsinger R L and Mirkin C A 1997 *Science* **277** 1078–81
- [25] Taton T A, Mirkin C A and Letsinger R L 2000 *Science* **289** 1757–60
- [26] Park S J, Taton T A and Mirkin C A 2002 *Science* **295** 1503–6
- [27] Cao Y W C, Jin R C and Mirkin C A 2002 *Science* **297** 1536–40
- [28] Tsai C Y, Chang T L, Chen C C, Ko F H and Chen P H 2005 *Microelectron. Eng.* **78/79** 546–55
- [29] Jung C, Mun H Y, Li T and Park H G 2009 *Nanotechnology* **20** 035607
- [30] Oaew S, Karoonuthaisiri N and Surareungchai W 2009 *Biosens. Bioelectron.* **25** 435–41
- [31] Zhang Y, Zhang K and Ma H 2009 *Am. J. Biomed. Sci.* **1** 115–25
- [32] Li Y, Qi H, Yang J and Zhang C 2009 *Microchim. Acta* **164** 69–76
- [33] Liu S F, Li Y F, Li J and Jiang L 2005 *Biosens. Bioelectron.* **21** 789–95
- [34] Friedberg E C 2003 *Nature* **421** 436–9
- [35] Futreal P A, Kasprzyk A, Birney E and Mullikin J C 2002 *Nature* **409** 850–2
- [36] Haiss W, Thanh N T K, Aveyard J and Ferning D G 2007 *Anal. Chem.* **79** 4215–24
- [37] Frens G 1972 *Colloid Polym. Sci.* **250** 736–41
- [38] Frens G 1973 *Nature* **241** 20–2
- [39] Luo Y 2007 *Mater. Lett.* **61** 1039–41
- [40] Shimizu T, Teranishi T, Hasegawa S and Miyake M 2003 *J. Phys. Chem. B* **107** 2719–24
- [41] Jana N R, Gearheart L and Murphy C J 2001 *Langmuir* **17** 6782–6
- [42] Lazarides A A and Schatz G C 2000 *J. Phys. Chem. B* **104** 460–7
- [43] Southern E M 1975 *J. Mol. Biol.* **98** 503–17
- [44] Mount D M 2004 *Bioinformatics: Genome and Sequence Analysis* (New York: Cold Spring Harbor Laboratory Press) p 34
- [45] Storhoff J J, Mucic R C, Mirkin C A, Letsinger R L and Schatz G C 2000 *J. Am. Chem. Soc.* **122** 4640–50